A Comparison of AC/DC Piezoelectric Transformer Converters with Current Doubler and Voltage Doubler Rectifiers

Gregory Ivensky, Svetlana Bronstein and Sam Ben-Yaakov*

Power Electronics Laboratory
Department of Electrical and Computer Engineering
Ben-Gurion University of the Negev
P. O. Box 653, Beer-Sheva 84105, ISRAEL,
Phone: +972-8-646-1561; Fax: +972-8-647-2949;
Email: sby@ee.bgu.ac.il; Website: www.ee.bgu.ac.il/~pel

***Abstract*.** **The objective of this study was to develop recommendations for an optimal design of PT AC/DC converters. The paper presents a comprehensive comparison of the two commonly used rectifier topologies in a piezoelectric transformer (PT) based power converters: current doubler and voltage doubler rectifiers. The advantages and disadvantages of the two rectifiers were investigated and the area of their applications with respect to output current, voltage, power capability, load resistance etc. - was delineated. Generic principles are proposed for choosing a PT for a given set of requirements, i.e. output voltage, input voltage and load resistance, as well the rectifier type suitable for the given PT and application. Simulation and experimental results support the theoretical study and are found to be in a good agreement with the analysis.**

I. Introduction

As Piezoelectric Transformer (PT) technology is developing, PTs may become a viable alternative to electromagnetic transformers in various applications such as power converters. Hence, the problem of optimal PT converter design becomes an important issue that needs to be addressed.

Two main types of rectifiers are generally applied at the output of PT AC/DC converters: the voltage doubler (VD) (Fig. 1a) and the current doubler (CD) (Fig. 1b).

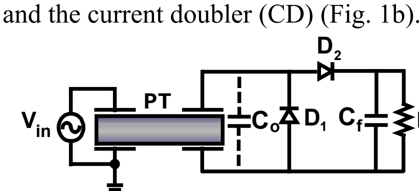

(a)

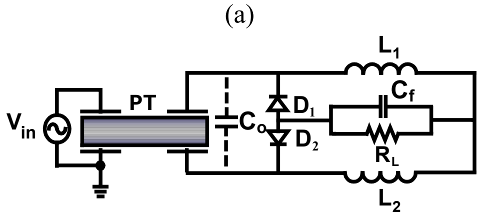

(b)

Fig. 1. Typical AC-DC PT power converter topologies: a) Voltage doubler rectifier , b) Current doubler rectifier. C_o is the output capacitance of the PT

* Corresponding author. This research was supported by THE ISRAEL SCIENCE FOUNDATION (grant No. 113/02) and by the Paul Ivanier Center for Robotics and Production management.

It is obvious that for high currents and low voltages (low resistance load) the CD rectifier is a superior choice, whereas for high voltages and low currents (high resistance load) the VD rectifier is a better choice. The problem is, however, that the load regions between these two rectification schemes are not well defined. This paper presents a comparative analysis of PT based power converters that apply these types of rectifiers. The objective of the study was to develop guidelines for optimal design of PT based AC/DC converter. The comparison methodology, applied in this study, follows the concept of representing the output capacitor of PT and the rectifier sections by an equivalent circuit [1-3]. The equivalent circuit is linear and is composed of a parallel RC network that loads the PT as the corresponding rectifier does [4,5]. The study uses the earlier generic analysis and generic characteristics of PT [6] together with the proposed comparative analysis of the two types of rectifiers for developing the generic model of PT AC/DC power converter.

II. The Comparative Circuits and the Comparison Principles

It is assumed that both converters are operated at the maximum output voltage mode, that is, at the frequency that produces the maximum output voltage. As was shown earlier [6], the frequency of maximum output is different from the mechanical resonant frequency. The principle of operation of the VD rectifier when operating at the maximum output voltage mode was studied in [4] and is further developed in the present work. Current doubler rectifier operating at the mechanical resonant frequency of PT was studied by number of investigations [1,5] while the present work studies its operation at the maximum output voltage mode.

In order to generalize the model of the PT converter we apply in this study the following normalized parameters:

Normalized load factor:

$$K_{PT}=R_L/n^2R_m \quad (1)$$

Normalized PT factor:

$$A_{PT}=\omega_r C_o n^2 R_m \quad (2)$$

PT mechanical quality factor:

$$Q_m=1/\omega_r C_r R_m \quad (3)$$

where R_L is the load resistance, R_m-L_r-C_r-C_o are the parameters of the equivalent circuit of PT; n is the PT's transfer ratio; and $\omega_r = 1/\sqrt{L_r C_r}$ is the mechanical resonant frequency of the PT.

The current and voltage waveforms of the rectifiers that are compared in the study are presented in Fig. 2. The parameters marked in Fig. 2 are defined as follows: $\vartheta = \omega t$ is the normalized time, ω is the operating angular frequency, θ is the duration of the VD rectifier input current pulses, λ is the duration of the CD rectifier input voltage pulses (i.e. the pulses of the output capacitor voltage).

The output voltage of the PT in both converters includes high harmonics components, whereas the current waveform within the PT equivalent circuit is assumed to be sinusoidal due to the high quality factor of the resonant circuit. Consequently, power transfer to the output is affected only by the fundamental harmonic component. For that reason, both rectifiers could be studied by the same fundamental harmonic method. In both converters we replace the output capacitor of the PT and the loaded rectifier by an equivalent parallel network C_{eq}-R_{eq} (at the secondary side of PT). In the case of ideal lossless rectifies these parameters are derived from:

$$\frac{V^2_{Co(1)pk}}{2R_{eq}} = \frac{V^2_L}{R_L} \tag{4}$$

$$C_{eq} = \frac{\tan\varphi_{(1)}}{\omega R_{eq}} \tag{5}$$

where $V_{Co(1)pk}$ is the peak of the first component of the capacitor C_o voltage v_{Co}, $\varphi_{(1)}$ is the phase angle between the voltage $v_{Co(1)}$ and the PT current i_r flowing through R_m-C_r-L_r.

Next we reflect this equivalent network to the primary (C'_{eq} - R'_{eq} are the reflected values) (Fig. 3a) where $C'_{eq} = C_{eq}n^2$, $R'_{eq} = R_{eq}/n^2$. This reflected parallel network is then converted to an equivalent series network C''_{eq} - R''_{eq} (Fig. 3b) [5, 6] by applying the following relationships:

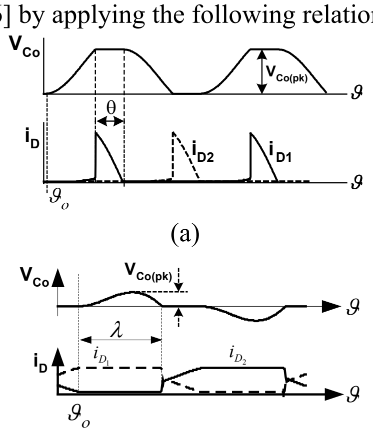

Fig. 2. The output voltage of the PT (across C_o) and the diodes currents: a) Voltage doubler rectifier, b) Current doubler rectifier

$$\begin{cases} R''_{eq} = R'_{eq}\cos^2\varphi_{(1)} \\ C''_{eq} = \dfrac{C'_{eq}}{\sin^2\varphi_{(1)}} \end{cases} \tag{6}$$

This presentation is used in the followings to obtain generalized expressions for the efficiency, power relationships, voltage ratio etc. in a similar form for the two converters. All expressions are normalized and apply per unit system.

2.1. Voltage Doubler Rectifier

Following [4], the duration of the impulses of the diodes' currents is θ (Fig. 2-a):

$$\theta \approx 2\tan^{-1}\sqrt{\frac{2\pi}{\omega C_o R_L}} = 2\tan^{-1}\sqrt{\frac{2\pi}{\Delta\omega q}} \tag{7}$$

where $q=\omega_r C_o R_L = A_{PT}K_{PT}$, $\Delta\omega=\omega/\omega_r$ is the ratio of the operating frequency ω to the mechanical resonant frequency of the PT ω_r [6] (operating frequency is assumed to be the frequency of maximum voltage transfer ratio:

$$\Delta\omega = \sqrt{1 + \frac{R_{eq}}{R_L}\frac{\sin^2\varphi_{(1)}}{A_{PT}K_{PT}Q_m}} \tag{8}$$

The waveform coefficient $k_{(1)}$ and the phase angle $\varphi_{(1)}$ of the first harmonics of the PT's output capacitance C_o voltage, referred to the instant $\vartheta_o = 0$ are:

$$k_{(1)} = \frac{V_{Co(1)pk}}{V_{Copk}} = \sqrt{a^2_{(1)} + b^2_{(1)}} \tag{9}$$

$$\varphi_{(1)} = \tan^{-1}\left(\frac{a_{(1)}}{b_{(1)}}\right) \tag{10}$$

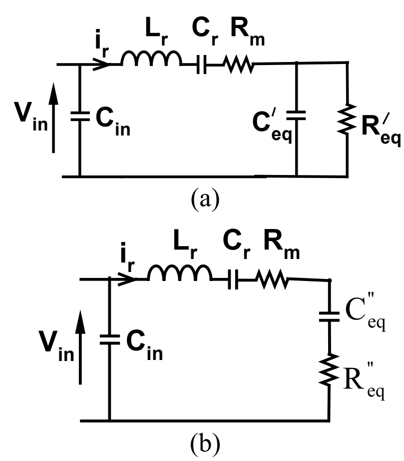

Fig. 3. Equivalent circuits of a PT AC-DC converter. The parallel C_{eq} and R_{eq} and series R_{eq}'' and C_{eq}'' networks emulate the loading effect of the rectifier (C_{eq} includes the output capacitance of the PT – C_o)

where V_{Copk} is the peak value of the voltage v_{Co} (Fig. 2), $a_{(1)}$ and $b_{(1)}$ are the first components of the Fourier series expansion:

$$a_{(1)} = -\frac{2}{\pi}\left[\frac{\pi - \theta + 0.5\sin(2\theta)}{1+\cos\theta}\right] \tag{11}$$

$$b_{(1)} = \frac{2}{\pi}(1-\cos\theta) \tag{12}$$

The equivalent resistance and capacitance are [4]:

$$\begin{cases} R_{eq}^{VD} = \frac{1}{8}k_{(1)}^2 R_L \\ C_{eq}^{VD} = \frac{\tan\varphi_{(1)}}{\omega R_{eq}^{VD}} \end{cases} \tag{13}$$

The voltage transfer function of the rectifier:

$$k_{rect} = \frac{V_L}{V_{Co(1)pk}} = \frac{2}{k_{(1)}} \tag{14}$$

2.2. CURRENT DOUBLER RECTIFIER

When connected to the output of the PT converter, the CD rectifier, as in the case of the halfway rectifier [5], can operate in overlapping (OM) or non-overlapping mode (NOM) with respect to the diodes' current.

Fig. 4 shows the waveforms of the PT current i_r/n (referred to the secondary side of the PT), and the input current to the rectifier, $i_{in(rect)}$ in the OM (Fig. 4a) and NOM (Fig. 4b).

We assume that the load current I_L and the inductors' L_1, L_2 currents have negligible ripple and therefore the waveform $i_{in(rect)}$ is clamped to the inductors' currents that are half the value of the load current. The difference between currents i_r/n and $i_{in(rect)}$ is the current of the PT output capacitor C_o.

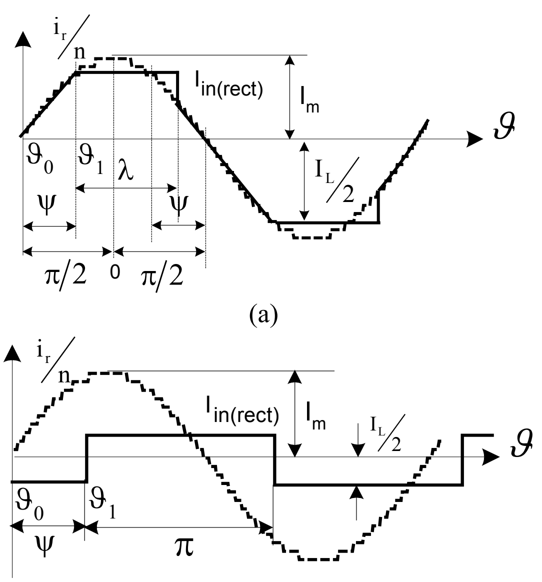

Fig.4. Current doubler rectifier input current (solid line) and a sinusoidal PT resonant current (dotted line) a – OM, b - NOM.

$$i_{Co} = I_m \sin\vartheta - 0.5 I_L \tag{15}$$

where $\vartheta=\omega_m t$ is normalized time referred to the instant ϑ_o (Fig. 4). This current charges and discharges the capacitor C_o during the time interval λ when the capacitor is not shorted through the conducting diodes. In OM (Fig. 4a), the capacitor current has no step at the instant ϑ_1 when the preceding overlapping period finishes. At this instant:

$$\frac{i_r}{n} = \frac{I_L}{2} = I_m \sin\psi \tag{16}$$

where ψ is defined in Fig. 4. In NOM (Fig. 4b) $i_{in(rect)}$ has a rectangular waveform. The steps of this current correspond to the instants when the capacitor voltage changes polarity

In steady state, the average charge during the time period λ is zero. Therefore in OM:

$$\int_{\psi}^{\psi+\lambda} (I_m \sin\vartheta - I_m \sin\psi)\, d\vartheta = 0 \tag{17}$$

The solution of this equation is:

$$\psi = \tan^{-1}\left(\frac{1-\cos\lambda}{\lambda - \sin\lambda}\right) \tag{18}$$

The voltage across C_o is obtained from (15), (16). Taking into account that $v_{Co}=0$ at $\vartheta=\psi$:

$$v_{Co} = \frac{I_m}{\omega C_o}\left[\cos\psi - \cos\vartheta + (\psi - \vartheta)\sin\psi\right] \tag{19}$$

The average output voltage of the rectifier is found from (19):

$$V_L = \frac{1}{2\pi}\int_{\psi}^{\psi+\lambda} v_{Co}\, d\vartheta \tag{20}$$

On the other hand:

$$V_L = I_L R_L = 2 I_m R_L \sin\psi \tag{21}$$

Combining (18)-(21) together we derive an important equation that connects the duration λ of the capacitor C_o voltage pulses with the parameter $q=\omega_r C_o R_L$:

$$\frac{0.5\lambda}{\tan(0.5\lambda)} = 1 - \sqrt{2\pi\omega C_o R_L} = 1 - \sqrt{2\pi q \Delta\omega} \tag{22}$$

The dependence of λ on q is depicted in Fig. 5.

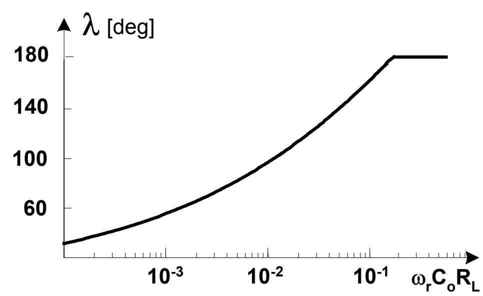

Fig. 5. Duration of the capacitor C_o pulses λ as a function of the parameter $q=\omega_r C_o R_L$

It follows from (22) that OM corresponds to the range of q values: $q < \frac{1}{2\pi}$.

Replacing the real voltage pulses v_{Co} by an equivalent sine wave with the same duration λ and the same peak $V_{Co(pk)}$ we define $k_{(1)}$, $\varphi_{(1)}$ and $V_L/V_{Co(pk)}$:

$$k_{(1)} = \frac{4}{\lambda}\frac{\cos\left(\frac{\lambda}{2}\right)}{\left(\frac{\pi}{\lambda}\right)^2 - 1} \quad (23)$$

$$\varphi_{(1)} = \psi + \lambda/2 - \pi/2 \quad (24)$$

$$\frac{V_L}{V_{Co(pk)}} = \frac{\lambda}{\pi^2} \quad (25)$$

Based on (4), (5), (9) and (25), the equivalent load resistance and capacitance in the OM (Fig. 4a) are:

$$\begin{cases} R_{eq}^{CD} = \frac{1}{2}\left(\frac{\pi^2}{\lambda}\right)^2 k_{(1)}^2 R_L \\ C_{eq}^{CD} = \frac{\tan\varphi_{(1)}}{\omega R_{eq}^{CD}} \end{cases} \quad (26)$$

In NOM (Fig. 4b) λ=π:

$$\frac{1}{\pi}\int_{\psi}^{\psi+\pi}\left(I_m \sin\vartheta - \frac{I_L}{2}\right)d\vartheta = 0 \quad (27)$$

It follows from this that:

$$\cos\psi = \frac{\pi}{4}\frac{I_L}{I_m} \quad (28)$$

$$\begin{cases} k_{(1)} = 1 \\ \varphi_{(1)} = \psi \end{cases} \quad (29)$$

$$\frac{V_L}{V_{Co(pk)}} = \frac{1}{\pi} \quad (30)$$

$$\omega C_o V_{Co(1)pk} = I_m \sin\psi \quad (31)$$

From (28), (30) and (31) we obtain:

$$\tan\psi = 4\omega C_o R_L = 4q \quad (32)$$

From (26) and (29) when λ=π, the equivalent resistance and capacitance in the NOM are found to be:

$$\begin{cases} R_{eq}^{CD} = \frac{\pi^2}{2} R_L \\ C_{eq}^{CD} = \frac{\tan\varphi_{(1)}}{\omega R_{eq}^{CD}} = \frac{8}{\pi^2} C_o \end{cases} \quad (33)$$

From (23) and (25) we obtain the voltage transfer ratio of the rectifier in OM:

$$k_{rect} = \frac{V_L}{V_{Co(1)pk}} = \frac{\lambda}{\pi^2 k_{(1)}} \quad (34)$$

In NOM (using (4), (29) and (30)):

$$k_{rect} = \frac{1}{\pi} \quad (35)$$

III. General Equations of a PT with a Rectifier at the Output

The PT voltage transfer function referred to the primary side of PT for both rectifiers is [6]:

$$k_{21m} = \frac{V_{Co(pk)}}{nV_{in(pk)}} = \frac{1}{\cos\varphi_{(1)} + \frac{1}{K_{PT}\cos\varphi_{(1)}}} \quad (36)$$

where $V_{in(pk)}$ is the peak input voltage.

The output to peak input voltage transfer ratio k_o is:

$$k_o = \frac{V_o}{V_{in(pk)}} = nk_{21m}k_{rect} \quad (37)$$

The efficiency of the PT for both rectifiers is given by [6]:

$$\eta_{PT} = \frac{1}{1 + \frac{R_m}{R''_{eq}}} = \frac{1}{1 + \frac{R_L}{n^2 K_{PT} R''_{eq}}} \quad (38)$$

The ratio of the output power to the power dissipation on PT for the both rectifiers is:

$$\Delta_{PT} = \frac{P_o}{P_{PT}} = \frac{\eta_{PT}}{1 - \eta_{PT}} = \frac{R''_{eq}}{R_L} K_{PT} \quad (39)$$

In the case of non-ideal rectifier one should take into account the diodes' losses.

The rectifiers' efficiency is:

$$\eta_{rect} = \frac{1}{1 + \frac{P_D}{P_o}} \quad (40)$$

where P_D is diodes' power losses and P_o is output power.

The diodes' power losses in both rectifiers are approximated by:

$$P_D = 2\left(I_{D(ave)}V_F + I_{D(rms)}^2 R_s\right) \quad (41)$$

where $I_{D(ave)}$ is the average diode current, V_F is the forward diode voltage, $I_{D(rms)}$ is the effective diode current and R_s is the diode's ohmic resistance. In the CD rectifier $I_{D(ave)}$=0.5I_L, where I_o is output voltage. In the VD rectifier $I_{D(ave)}$=I_L

The efficiency of the rectifiers when connected at the PT output is found to be:

$$\eta_{rect}^{CD} \approx \frac{1}{1 + \frac{V_F}{V_L}\left[1 + \left(\frac{I_{D(rms)}}{I_{D(ave)}}\right)^2 \frac{V_L}{V_F}\frac{R_s}{2R_L}\right]} \quad (42)$$

$$\eta_{rect}^{VD} = \frac{1}{1 + \frac{2V_F}{V_L}\left[1 + \left(\frac{I_{D(rms)}}{I_{D(ave)}}\right)^2 \frac{V_L}{V_F}\frac{R_s}{R_L}\right]} \tag{43}$$

where $\frac{I_{D(rms)}}{I_{D(ave)}}$ is the ratio of rms and the average diodes' currents:

$$\left.\frac{I_{D(rms)}}{I_{D(ave)}}\right|_{CD} = \sqrt{\frac{1}{\pi}\left\{\left[\frac{\lambda^2}{\pi^2} + \frac{2}{3}\left(1 - \frac{\lambda^2}{\pi^2}\right)^2\right](\pi - \lambda) + \lambda\right\}} \tag{44}$$

$$\left.\frac{I_{D(rms)}}{I_{D(ave)}}\right|_{VD} = \sqrt{\frac{\pi\left[\theta - \frac{1}{2}\sin(2\theta)\right]}{[1 - \cos(\theta)]^2}} \tag{45}$$

Taking into account the rectifier losses, the overall efficiency will be:

$$\eta = \eta_{rect}\eta_{PT} \tag{46}$$

IV. Main Comparison Results

Fig. 6, that is based on (38), (39) shows the power handling capability Δ_{PT} as a function of the normalized load factor $K_{PT}=R_L/n^2R_m$ for different values of the normalized PT parameter $A_{PT}=\omega_r C_o n^2 R_m$. Since the efficiency equals $\Delta_{PT}/(\Delta_{PT}+1)$ the maximum of Δ_{PT} corresponds to the point of maximum efficiency. The generic data of Fig. 6 suggest that for any given PT (i.e. a specific A_{PT}) the efficiency that can be achieved with a CD rectifier is higher than the one that can be reached with the VD rectifier. The data also show, as expected, that for a given PT, the load R_L that corresponds to maximum efficiency, is lower in the CD rectifier than in the VD rectifier. That is, maximum efficiency will be obtained in the VD rectifier at higher voltages than in the CD rectifier. From Fig. 6 one can recognize the borderline between load values that will produce a higher efficiency with a CD rectifier, to the load range that is more compatible to the VD rectifier (from the efficiency point of view). Fig. 7, built from Fig. 6, delineates the borderline between the CD and VD regions for different PT's for a range of A_{PT} values. This plot can be used as a tool for selecting the rectifier for a given load conditions of a given PT. This figure implies that, for a given PT, one should use a VD rectifier when the load factor ($R_L/n^2 R_m$) is higher then the dotted line, and CD – when the load factor is lower. The plots (Fig. 6-7) are built for mechanical quality factor of PT Q_m=900. t was found, however, that Δ_{PT} does not changed significantly when Q_m>900.

If the high voltage gain is to be achieved in a given application, it follows from (9), (14) and (23), (34), (35) that VD has higher k_{rect} than CD, therefore VD is better choice for a given PT.

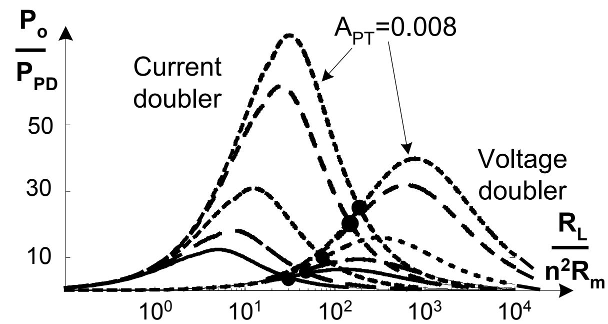

Fig. 6. The ratio of the output power P_o to the PT power dissipation P_{PD} (Δ_{PT}) as a function of the normalized load resistance $K_{PT}=R_L/n^2R_m$ for different PT factor $A_{PT}=\omega_r C_o R_m n^2$ (from top to bottom A_{PT}=0.008, 0.01, 0.02, 0.034, 0.05). Plots are for mechanical quality factor Q_m=900.

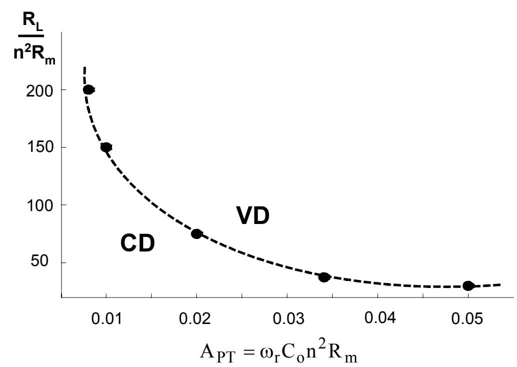

Fig. 7. Boundary conditions for the choosing the rectifier type (factor $A_{PT}=\omega_r C_o n^2 R_m$) for achieving better efficiency according to the application (normalized load factor $K_{PT}=R_L/n^2R_m$). Mechanical quality factor Q_m=900.

It is further found in this study that for low load resistances, higher voltage transfer ratios can be obtained when using the CD rather than the VD rectifier (Fig. 8). This is because the efficiency of CD with low load resistances is higher than the VD. In addition, the diodes' efficiency of CD is higher than VD, because the ratio of $I_{D(rms)}/I_{D(ave)}$ in the CD is lower than in the VD.

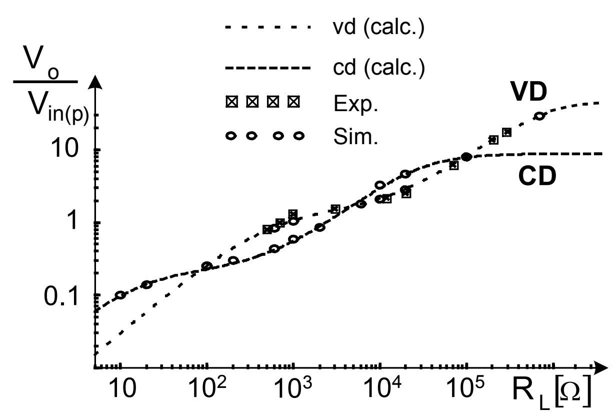

Fig. 8. Output to input voltage ratio of the PT converter for the two rectifiers' types. (For PT Philips, RT 35x8x2 PXE43-S).

V. Simulation and Experimental Results

The experimental transformer was a thickness vibration mode PT (Philips, RT 35x8x2 PXE43-S). The parameters of the simplified electrical equivalent circuit were measured to be: series inductance L_r=165mH, series capacitance C_r=15.1pF, output capacitance C_o=510pF, loss resistance R_m=105Ω, mechanical transfer ratio n=1.

It was assumed that the required output voltage is constant. Figs. 8-10 show the simulation and the experimental results as well as the calculated results according to the model presented here, as a function of the load resistance for the given PT: the output to input voltage transfer ratio (Fig. 8), the ratio of the output power to the power dissipation on PT (Fig. 9) and the converter efficiency (Fig. 10) (for the voltage doubler rectifier). In this case the maximum efficiency that was achieved with the experimental PT was approximately 90% (Fig. 10).

VI. Conclusion

This study carries out a comprehensive comparison of two popular rectifiers in PT power converter: a current doubler and a voltage doubler. The advantages and disadvantages of each rectifier configuration were studied resulting in a recommendation of the preferred applications areas for each rectifier in terms of output current and voltage, power handling capability, load resistance etc.

The results of this study are general and are not confined to any particular PT since we apply here generic parameters for the PT and load. The PT is characterized by the normalized parameters: A_{PT}, Q_m, and n, while the load is expressed in a normalized form as K_{PT}. These fundamental parameters are used to develop the relationship for the maximum voltage transfer function and Δ_{PT} that is the ratio of the output power to the power dissipated by the PT. Since the maximum allowable PT power dissipation is one of the most important design constrains, the value of the parameter Δ_{PT} in any given application will determine what would be the maximum output power of the system.

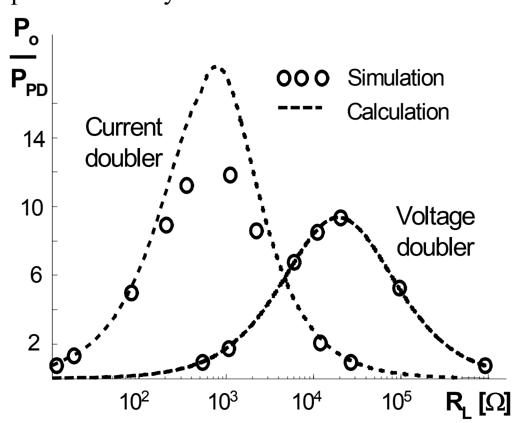

Fig. 9. Ratio of the output power P_o to the power dissipation of the PT P_{PD} as a function of the load resistance R_L. (The same PT)

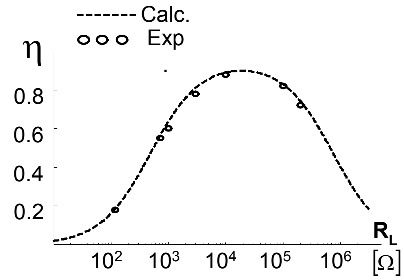

Fig. 10. Efficiency of a PT converter with a voltage doubler rectifier as a function of the load resistance. (The same PT)

The study shows that a higher maximum overall efficiency can be achieved when applying a current doubler than when a voltage doubler rectifier is used. It is further found in this study that for low load resistances, higher voltage transfer ratios can be obtained when using the CD rather than the VD rectifier whereas for achieving high gain the VD rectifier is much more suitable (Fig. 8).

In general, the simulations and the experiments confirm the theoretical analysis and were found to be in a good agreement. The discrepancies that are observed in some cases are probably due to experimental error. For example, the larger errors close to the peak of Δ_{PT} in Fig. 9 are explained by the fact that the peak of maximum efficiency also corresponds to the minimum point in the power transfer curve (for a constant input voltage) [6]. Consequently, the relative error due to parasitic effects (such as unaccounted for diodes and inductor losses) is expected to be large.

The analytical methodology developed and applied in this paper and the closed form analytical expressions that were derived, provide generic information on PT converter that apply the CD and VD rectifiers. The analytical expressions that are also summarized in generic graphs, shed some more light on characteristics and advantages and disadvantages of PTs. As such, they could be useful both ways: when selecting a PT for a given application and when designing a PT for a specific system.

References

[1] C. Y. Lin and F. C. Lee, "Design of a Piezoelectric Transformer Converter and Its Matching Networks," *IEEE PESC Record*, pp. 607-612, 1994.
[2] R. L. Steigerwald, "A Comparison of Half-Bridge Resonant Converter Topologies," *IEEE Trans. On Power Electronics*, Vol. 3, no. 2, pp. 174-182, Apr. 1988.
[3] G. Ivensky, A. Kats, and S. Ben-Yaakov, "An RC Load Model of Parallel and Series-Parallel Resonant Converters with Capacitive Output Filter," *IEEE Trans. On Power Electronics,* vol. 14, no. 3, pp. 515-521, May 1999.
[4] G. Ivensky, M. Shvartsas, and S. Ben-Yaakov, "Analysis and Modeling of a Piezoelectric Transformer in High Voltage Applications," *IEEE APEC'2000 Record*, pp. 1081-1087.
[5] G. Ivensky, S. Bronstein, and S. Ban-Yaakov, "Analysis and Design of a Piezoelectric Transformer AC/DC Converter in a Low Voltage Application," *IEEE PESC'2002 Record*, pp. 409-414.
[6] G. Ivensky, I. Zafrany, and S. Ban-Yaakov, "Generic Operational Characteristics of Piezoelectric Transformers," *IEEE Trans. On Power Electronics*, Nov. 2002, vol. 17, no 6, pp. 1049-1057.